trical resistance and diamagnetism in superconductors above their transition temperatures.

Note added.—Following a suggestion by Professor Maki, we find that an excellent fit to the experimental data shown in Figs. 1 and 2 for the excess ultrasonic attenuation over that extrapolated for normal zero sound is

$$[\alpha_0/(\alpha_0)_c]_{\text{excess}} = 0.07_6 - 0.327(T/T_c - 1)^{1/2},$$

for $(T/T_c - 1) > 0$. Below the transition temperature, $1.2\times10^{-3} > (1 - T/T_c) > 5\times10^{-5}$, the excess attenuation is fitted by

$$[\alpha_0/(\alpha_0)_c]_{\text{excess}} = 0.090 + 3.9\times10^2(1 - T/T_c).$$

For $5\times10^{-5} > (1 - T/T_c) > 0$, the excess attenuation rises somewhat more rapidly than this formula suggests.

This work was supported by the U. S. Department of Energy under Contract No. EY-76-S-03-0034, P. A. 143.

[1] L. D. Landau, Zh. Eksp. Teor. Fiz. 32, 59 (1957) [Sov. Phys. JETP 5, 101 (1957)].

[2] A. A. Abrikosov and J. M. Khalatinkov, Zh. Eksp. Teor. Fiz. 33, 110 (1967) [Sov. Phys. JETP 6, 84 (1958)].

[3] W. R. Abel, A. C. Anderson, and J. C. Wheatley, Phys. Rev. Lett. 17, 74 (1966).

[4] D. N. Paulson, R. T. Johnson, and J. C. Wheatley, Phys. Rev. Lett. 30, 829 (1973).

[5] D. N. Paulson, H. Kojima, and J. C. Wheatley, Phys. Lett. 47A, 457 (1974).

[6] J. M. Parpia, D. J. Sandiford, J. E. Berthold, and J. D. Reppy, Phys. Rev. Lett. 40, 565 (1978).

[7] D. J. Thouless, Ann. Phys. (N.Y.) 10, 533 (1960).

[8] V. J. Emery, Ann. Phys. (N.Y.) 28, 1 (1964).

[9] V. J. Emery, J. Low Temp. Phys. 22, 467 (1976).

[10] M. Tinkham, Rev. Mod. Phys. 46, 587 (1974).

[11] M. Krusius, D. N. Paulson, and J. C. Wheatley, to be published.

[12] D. N. Paulson, M. Krusius, and J. C. Wheatley, to be published; R. S. Safrata, M. Koláč, T. Těthal, K. Svec, and J. Matas, to be published.

[13] J. C. Wheatley, Rev. Mod. Phys. 47, 415 (1975).

[14] E. Egilsson and C. J. Pethick, J. Low Temp. 29, 99 (1978).

[15] For a review, see J. C. Wheatley, in "Progress in Low Temperature Physics" (to be published), Vol. VII.

[16] D. N. Paulson and J. C. Wheatley, unpublished.

[17] For a review, see P. Wölfle in "Progress in Low Temperature Physics" (to be published), Vol. VII.

Thermorotation Effects in Superfluid Helium

E. J. Yarmchuk and W. I. Glaberson
Department of Physics, Rutgers University, New Brunswick, New Jersey 08903
(Received 16 June 1978)

We have observed a variety of thermorotation effects, effects involving thermal counterflow in rotating superfluid helium. In particular, the temperature and chemical-potential gradients associated with the motion of vortex lines have been measured.

It is generally believed that dissipative superfluid flow is associated with the motion of vortices through the superfluid.[1] Anderson[2] has pointed out that vortices crossing a line connecting two points at rest in the superfluid produce a chemical-potential difference between the two points proportional to the rate of crossing. This is a consequence of an "ac Josephson effect" in helium in which a chemical-potential difference is proportional to the rate at which the order-parameter phase difference changes—each vortex passage producing a phase change of 2π. There have been a number of experiments[3] which demonstrate that vorticity is associated with turbulent counterflow or pressure-driven flow but these experiments are impossible to directly relate to Anderson's prediction. There is evidence[4] that charged vortex rings pushed towards an orifice connecting two baths can produce a level difference between the baths. This, however, is a situation in which there is no dissipative superflow and, in any event, quantitative confirmation of Anderson's prediction is lacking. In this Letter, we describe a series of experiments in which an array of parallel vortex lines is moved through the fluid in a relatively controlled manner and the resultant temperature and chemical-potential gradients are observed. In addition, we report the observation of a number of interesting effects associated with the fact that the vortex array is confined within a channel of finite dimensions.

Consider an array of straight parallel vortex lines in the presence of thermal counterflow transverse to the lines.[5] One can easily show that chemical-potential gradients with components both along the counterflow as well as perpendicular to it are set up. One way of visualizing this effect is to consider a single vortex line. In the presence of transverse counterflow the line will, in general, experience frictional forces both along the counterflow and perpendicular to it. The line will then move with velocity $\vec{V}_L$ at an angle with respect to the counterflow in such a way that the magnus force produced by the relative motion between the line and the superfluid exactly balances the frictional forces. A chemical potential gradient is then set up perpendicular to $\vec{V}_L - \vec{V}_S$. An analogous effect was observed[6] in superconductors in which chemical-potential gradients were observed in a type-II superconducting film in a magnetic field in the presence of a heat current transverse to the flux lines.

Our experimental arrangement, shown schematically in Fig. 1, involves a glass channel of rectangular cross section, closed at one end with the other end open to a pumped helium bath. A resistive heater is placed near the closed end and the channel is rotated about a vertical axis perpendicular to the heat current. The channel investigated was of large aspect ratio, the height being 0.5 mm, the width 1.4 cm, and the length $5\frac{1}{2}$ cm. Temperature sensors were aluminum films, held in their superconducting transition regions ($T \sim 1.3$ K), evaporated onto one of the glass channel walls. The sensors were placed in the middle of the channel, approximately 1 cm apart, and separated on a line at an angle of $\sim 45°$ with respect to the channel axis. The sensitive thermometric technique required in these experiments, having a temperature-difference noise level of ~ 40 ndeg/Hz$^{1/2}$, is described elsewhere.[7] Temperature differences were measured in both clockwise and counterclockwise rotations and the components of the temperature gradients parallel and perpendicular to the heat current were obtained. Under the conditions of our experiment, both components were of similar magnitude.

Direct chemical-potential measurements were obtained by means of a differential pressure transducer. One side of the transducer was open to the bath and the other side was connected through a superleak to an opening in one of the channel walls between the heater and the closed end of the channel. The transducer, utilizing a

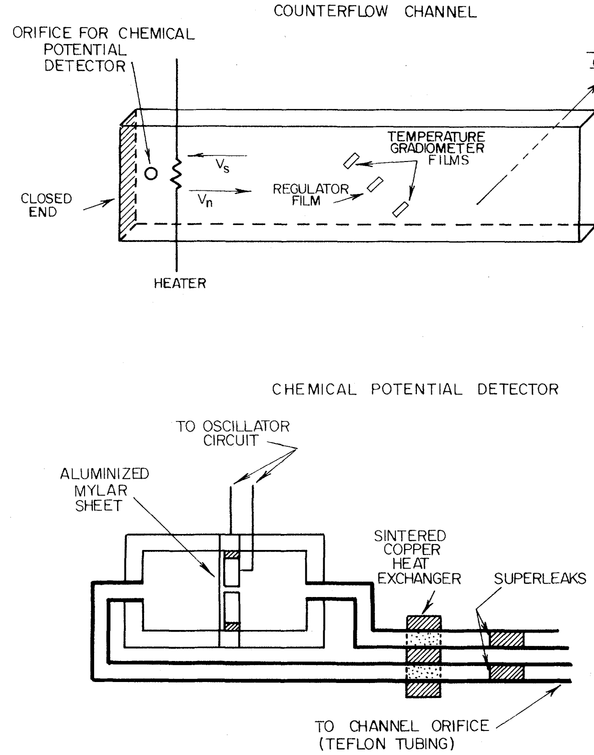

FIG. 1. A schematic drawing of the counterflow channel and chemical-potential detector. Of the three aluminum films, the center one is used to regulate the ambient bath temperature and the outer two are used in a bridge as temperature-difference detectors.

stretched aluminized Mylar sheet as one side of a capacitor in a tunnel-diode oscillator circuit,[8] had a noise level of about 10^{-3} dynes/cm^2 Hz$^{1/2}$. The transducer was thermally isolated from the channel by the superleak and thermal coupling between the two sides of the transducer was accomplished by means of a sintered copper heat exchanger. The effect of thermal isolation from the channel and thermal coupling across the transducer is to convert chemical-potential differences to pure pressure differences detected by the transducer.

The parallel component of the temperature gradient is shown in Fig. 2 as a function of heater power for several rotation speeds. We note that (a) the temperature gradients in the linear (nonturbulent) regimes increase as the rotation speed is increased, (b) the critical heater power Q_{c2}, associated with the onset of turbulent counterflow,[9] is increased as the rotation speed is increased[10]—apparently becoming proportional to $\sqrt{\Omega}$ as Ω gets large, (c) turbulent onset is characterized by a relatively smooth deviation from

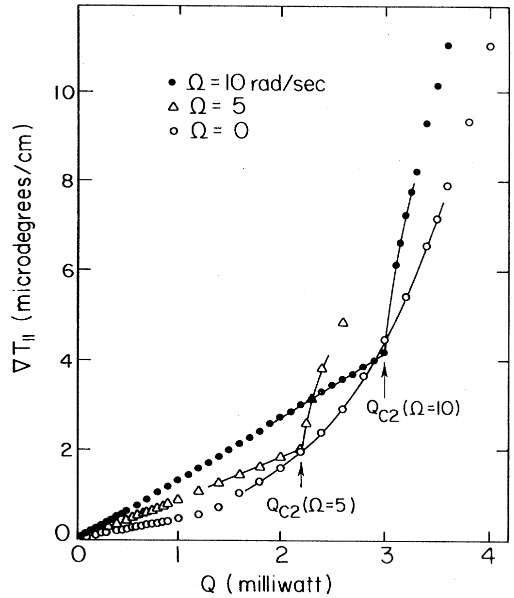

FIG. 2. A plot of the parallel component of the temperature gradient vs heater power for several rotation speeds. The solid lines are an aid to the eye.

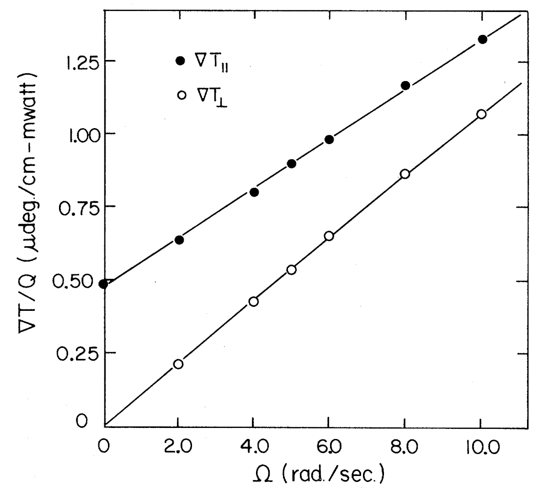

FIG. 3. A plot of $\nabla T_{\parallel}/Q$ and $\nabla T_{\perp}/Q$ in the linear regime vs rotation speed. The solid lines are fits to the theory as discussed in the text.

linearity when not rotating but by a sharp change of slope when rotating, (d) turbulent onset occurs at a heater power close to the power where the laminar-flow temperature gradients would cross the nonrotating turbulent curve, and (e) the temperature gradient in the fully turbulent regime ($Q \gg Q_{c2}$) differs from that in the nonrotating situation by an amount which becomes Ω independent as Ω gets large.

A plot of the linear-regime slopes versus rotation speed for both parallel and perpendicular components of the temperature gradient are shown in Fig. 3. Hall's two-fluid equations for the rotating superfluid[11] can be solved explicitly for the temperature and pressure gradients in terms of the mutual friction coefficients. In an infinite medium, the chemical-potential gradient manifests itself as a pure temperature gradient.[12] The solid lines are fits to the data using a solution to the equations for a channel of infinite aspect ratio. The values of the mutual friction coefficients obtained from this fit are in reasonable agreement with those previously measured.[13] The two-fluid equations for a channel are incomplete and a unique solution can only be obtained by introducing a boundary condition on the tangential component of $\vec{V}_s$ or of $\nabla\times\vec{V}_s$. We chose to specify that the components of $\nabla\times\vec{V}_s$ perpendicular to the rotation axis are zero at the boundaries for the purpose of fitting the data. The boundary conditions involved are macroscopic and should not be confused with microscopic boundary conditions involving isolated vortex lines intersecting walls.

Because we wished to observe, without ambiguity, the presence of a chemical-potential gradient associated with the vortex motion, and because we wished to extend the measurements to different temperatures, we introduced the chemical-potential detector discussed earlier. For reasons which we do not fully understand, noise problems prevented us from inserting the probe in the counterflowing region. Perhaps the orifice disturbed the flow in its vicinity sufficiently to cause vortices to nucleate or at least to hang up there in such a way as to cause large fluctuations in the chemical-potential difference across the orifice. In placing the probe behind the heater, we seem to have completely avoided this difficulty. We found that all of the effects (a)–(e) discussed above were observed with respect to chemical potential at all temperatures investigated ($1.15\ \mathrm{K} < T < 2.17\ \mathrm{K}$).

A plot of the chemical-potential gradient $\nabla\mu$ versus heater power Q for $\Omega = 0$ and $\Omega = 10$ rad/sec is shown in Fig. 4.[14] Also shown for comparison is the temperature gradient. Note that there exists a critical heater power Q_{c1}, not observable in the temperature measurements, below which $\nabla\mu$ is zero. We associate Q_{c1} with the power at which the vortex array "depins" and begins to move in response to the counterflow. Below Q_{c1}, the vortices are pinned to protuber-

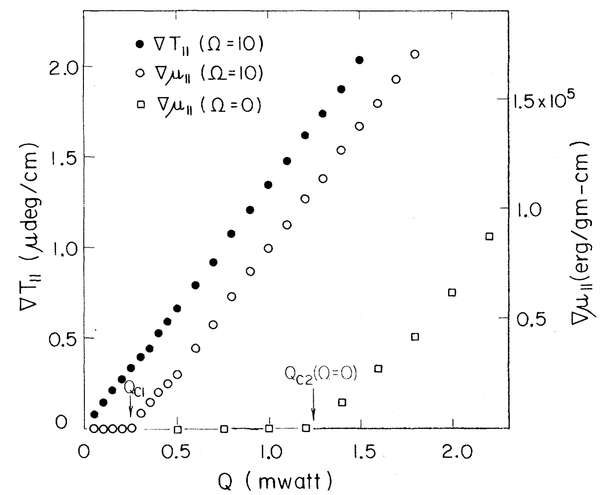

FIG. 4. A plot of the chemical-potential gradient and temperature gradient vs heater power for $\Omega = 0$ and $\Omega = 10$ rad/sec.

ances in the channel walls and accommodate the counterflow by deforming. If we adjust the boundary condition on $\nabla \times \vec{V}_s$ in the calculation so as to produce no longitudinal chemical-potential gradient, we find that, indeed, little influence on ∇T is predicted—the pressure gradient does, of course, become large. We observed that Q_{c1} is weakly Ω dependent, becoming smaller as Ω is increased. We suggest that it is unlikely that individual vortices in the array will move without the others and that Q_{c1} is associated with some average pinning force. Clearly, the largest protuberances will be the first to be occupied by vortices so that as the vortex density is increased, the average pinning force will decrease. We cannot, however, rule out an explanation of the Ω dependence of Q_{c1} in terms of mechanical vibration levels of the apparatus. Note that at Q_{c1}, at 1.3 K, the superfluid velocity is only 0.02 cm/sec. A crude estimate based on this velocity gives a depinning force of about 10^{-7} dynes per line.

The actual flow pattern in the region below Q_{c2} is quite interesting. A solution of the Hall equation yields a secondary flow in which an element of normal fluid executes a counterclockwise spirallike motion if in the upper half of the channel and a clockwise spirallike motion if in the lower half of the channel. The superfluid behaves similarly although in the opposite direction, of course. This sort of pattern is similar to the behavior in the flow of ordinary fluids in rotating channels.[15] An increase in the critical Reynolds number for ordinary fluids in a rotating channel has also been observed.[16] This increase for both ordinary fluids and the superfluid can probably be explained as a consequence of the Taylor-Proudman theorem[17] which tends to make a rotating fluid more stable with respect to three-dimensional perturbations.

This work was supported in part by a grant from the National Science Foundation.

[1]See, e.g., R. P. Feynman, in *Progress in Low Temperature Physics*, edited by C. J. Gorter (North-Holland, Amsterdam, 1955), Vol. 1, Chap. II, p. 45.

[2]P. W. Anderson, Rev. Mod. Phys. 38, 298 (1969).

[3]See, e.g., G. Careri, in *Progress in Low Temperature Physics*, edited by C. J. Gorter (North-Holland, Amsterdam, 1961), Vol. III, Chap. II, p. 66; G. Gamota, Phys. Rev. Lett. 31, 517 (1973).

[4]R. Carey, B. S. Chandrasekhar, and A. J. Dahm, Phys. Rev. Lett. 31, 873 (1973).

[5]The situation in which the counterflow is parallel to the lines is discussed in W. I. Glaberson, W. W. Johnson, and R. M. Ostermeier, Phys. Rev. Lett. 33, 1197 (1974), and R. M. Ostermeier and W. I. Glaberson, J. Low Temp. Phys. 21, 191 (1975).

[6]E. K. Sichel and B. Serin, J. Low Temp. Phys. 3, 635 (1970).

[7]E. J. Yarmchuk and W. I. Glaberson, Rev. Sci. Instrum. 49, 460 (1978).

[8]The circuit is similar to that described in C. T. Van Degrift, Rev. Sci. Instrum. 45, 1171 (1974).

[9]Our value for the critical velocity at $\Omega = 0$, scaled as the reciprocal of the height of the channel, agrees, within mutual uncertainties (~ 10%), with the data of R. K. Childers and J. T. Tough, Phys. Rev. B 13, 1040 (1976).

[10]This result is in clear disagreement with that of Chase [C. E. Chase, in *Proceedings of the Seventh International Conference on Low Temperature Physics*, edited by G. M. Graham and A. C. Hollis Hallet (Univ. of Toronto Press, Toronto, 1966), p. 438]. Chase's results were based on an experimental technique involving the rate at which dissipation developed and was not a direct measurement of critical counterflow velocity. The sensitivity of his technique did not allow an observation of the laminar-flow regime.

[11]H. E. Hall, in *Liquid Helium, Proceedings of the International School of Physics "Enrico Fermi" Course XXI*, edited by G. Careri (Academic, New York, 1963).

[12]The solution to the Hall equations being $\nabla T_{\parallel} = (\rho_n \Omega q/\rho_s \rho S^2 T)B$, $\nabla T_{\perp} = (\rho_n \Omega q/\rho_s \rho S^2 T)(2 - B')$, $\nabla P = 0$ where ρ_n, ρ_s, and ρ are the normal-fluid, superfluid, and total densities, respectively, Ω is the rotation speed, q is the heat flux density, S is the specific entropy, and B and B' are the mutual friction coefficients. In a channel of finite height, the solutions are much more complex and both temperature and pressure gradients

are present.

[13]We find $B = 1.47 \pm 0.15$ and $2 - B' = 1.8 \pm 0.2$ at $T = 1.3$ K. These agree within our mutual uncertainties, with an extrapolation of the data in P. Lucas, J. Phys. C 3, 1180 (1970), to our temperature.

[14]Strictly speaking, what is plotted is the average chemical-potential gradient between the heater and the open end of the channel. No attempt was made to account for inlet or outlet effects.

[15]G. S. Benton and D. Boyer, J. Fluid Mech. 26, 69 (1966); D. A. Bennetts and L. M. Hocking, Phys. Fluids 17, 1671 (1974).

[16]H. Ito and K. Nanbu, J. Basic Eng. 93, 383 (1971).

[17]G. I. Taylor, Proc. Roy. Soc., Ser. A 100, 114 (1921); J. Proudman, Proc. Roy. Soc., Ser. A 92, 408 (1916).

Theory of the Neutron Scattering Cross Section in Spin-Glasses

C. M. Soukoulis, G. S. Grest, and K. Levin

The James Franck Institute and the Department of Physics, The University of Chicago, Chicago, Illinois 60637

(Received 2 March 1978)

Using mean-field theory we compute the frequency-integrated neutron cross section $I(q,T)$ for spin-glasses. We find, as observed experimentally, that the temperature of the maximum of $I(q,T)$ depends on the momentum transfer q and is different from the freezing temperature T_c at which the susceptibility $\chi(q,T)$ has a cusp. These results suggest that recent neutron scattering experiments are consistent with a sharp phase transition at a single temperature T_c in spin-glasses.

Among the more puzzling experimental results concerning the concentrated spin-glass alloys are Murani's recent neutron scattering measurements,[1] which show that the frequency-integrated scattering intensity $I(q, T)$ has a temperature-dependent maximum which varies with momentum transfer q. These data have been interpreted[1] as suggesting that there is no unique freezing temperature in these alloys, associated with the spin-glass phase. Rather, the system is viewed as subdivided into correlated, ferromagnetic clusters, which freeze at different temperatures depending on their characteristic size.

The purpose of the present Letter is to show that these neutron experiments *are* consistent with the theory that there is a sharp phase transition in the spin-glasses. This is demonstrated in two different ways based on (i) a simple data analysis and (ii) a mean-field random-phase-approximation (RPA) calculation of the neutron scattering cross section, appropriate to concentrated spin-glasses.

The frequency-integrated neutron scattering cross section is given by[2]

$$\frac{d\sigma}{d\Omega_q} = \frac{N}{\hbar}\left(\frac{\gamma e^2}{mc^2}\right)^2 \frac{k'}{k} |F(q)|^2 I(q, T). \tag{1}$$

Here N is the number of scattering sites, k and k' are the incident and final wave vectors of the neutron, $\gamma e^2/mc^2$ is the coupling constant, and $F(q)$ is the scattering form factor which varies on a scale characteristic of atomic dimensions. The quantity $I(q, T)$ is given by

$$I(q, T) = N^{-1} \sum_{i,j} [\langle \vec{S}_i \cdot \vec{S}_j \rangle]_c \exp[i\vec{q} \cdot (\vec{R}_i - \vec{R}_j)], \tag{2}$$

where $[\,]_c$ denotes a configuration average and it is assumed that, consistent with experiment,[1] the magnetic contribution dominates that of potential scattering. $I(q, T)$ is generally written as

$$I(q, T) = k_B T \chi(q, T) + I_B(q, T), \tag{3}$$

where k_B is the Boltzmann's constant. We thus define

$$k_B T \chi(q, T) \equiv N^{-1} \sum_{i,j} \{[\langle \vec{S}_i \cdot \vec{S}_j \rangle]_c - [\langle \vec{S}_i \rangle \cdot \langle \vec{S}_j \rangle]_c\} \exp[i\vec{q} \cdot (\vec{R}_i - \vec{R}_j)], \tag{4a}$$

and

$$I_B(q, T) \equiv N^{-1} \sum_{i,j} [\langle \vec{S}_i \rangle \cdot \langle \vec{S}_j \rangle]_c \exp[i\vec{q} \cdot (\vec{R}_i - \vec{R}_j)]. \tag{4b}$$

This last term plays a role analogous to the Bragg scattering term in ordinary ferromagnets, whereas

